

# VELOCITY TRENDS IN THE DEBRIS OF SAGITTARIUS AND THE SHAPE OF THE DARK-MATTER HALO OF THE GALAXY

AMINA HELMI<sup>1</sup>

Kapteyn Institute, P.O. Box 800, 9700 AV Groningen, The Netherlands

*Draft version November 15, 2018*

## ABSTRACT

Recently, radial velocities have been measured for a large sample of M giants from the 2MASS catalog, selected to be part of the Sgr dwarf leading and trailing streams. Here we present a comparison of their kinematics to models of the Sgr dwarf debris orbiting Galactic potentials, with halo components of varying degrees of flattening and elongation. This comparison shows that the portion of the trailing stream mapped so far is dynamically young and hence does not provide very stringent constraints on the shape of the Galactic dark-matter halo. The leading stream, however, contains slightly older debris, and its kinematics provide for the first time direct evidence that the dark-matter halo of the Galaxy has a prolate shape with an average density axis ratio within the orbit of Sgr close to 5/3.

*Subject headings:* dark-matter – Galaxy: halo, kinematics and dynamics, structure, fundamental parameters

## 1. INTRODUCTION

Using M giant candidates from the 2MASS catalog, Majewski et al. (2003) have been able to trace streams from the Sagittarius dwarf through roughly 360 degrees on a great circle on the sky. More recently, the radial velocities of a subset of several hundred of these M giant candidates have been measured. The results have been presented in Law et al. (2003) and in tabular form (for the trailing stream) in Majewski et al. 2004 (hereafter M04). Hence 4 of the 6 phase-space coordinates of the stars in the streams are now available for a comprehensive dynamical study.

One of the intriguing questions that can in principle be addressed with such a dataset, concerns the shape of the dark-matter halo of the Galaxy. Is this flattened? Prolate or oblate? Ibata et al. (2001) and Majewski et al. (2003) have argued that the fact that the debris of Sgr is distributed along an almost complete great circle on the sky implies that the dark halo of the Milky Way has to be very close to spherical, with allowed (density) axis ratios in the range 0.9 to 1 (Law et al. 2003). On the other hand, Helmi (2004) has shown that, if the debris discovered so far is made up of material lost in the last 3 to 4 pericentric passages (i.e. less than 3 Gyr ago), then such debris would also be found along a great circle on the sky. Flattened (oblate) or elongated (prolate) halos with average density axis ratios, measured within the region probed by the debris, that are as low as 3:5 or as high as 5:3, respectively, would be allowed. Such values would be consistent with those found in numerical simulations of cold dark-matter halos (e.g. Bullock 2002).

The motivation behind this Letter is to establish whether the additional kinematic information that has now become available could perhaps break this degeneracy and allow us to better constrain the axis ratio of the Galaxy’s dark-matter halo.

## 2. COMPARISON OF MODELS AND DATA

The models presented here are more thoroughly discussed in Helmi (2004). Now we only present a brief summary. We have performed numerical simulations of the disruption of a system like the Sgr dwarf orbiting a Galactic potential with 3 components: a bulge, a disk and a dark logarithmic halo

$$\Phi_{\text{halo}} = v_{\text{halo}}^2 \ln(R^2 + z^2/q^2 + d^2), \quad (1)$$

where  $d = 12$  kpc and  $v_{\text{halo}} = 131.5$  km/s (Johnston et al. 1996). The parameter  $q$  is allowed to vary from 0.8 to 1.25, that is, from an oblate to a prolate configuration<sup>2</sup>. The satellite galaxy is modeled by a set of 50000 self-gravitating particles. We use a quadrupole expansion of the internal potential of the system, and choose a King profile for the pre-disruption dwarf. The orbital initial conditions are chosen to satisfy the constraints given by the present position and radial velocity of the main body of Sgr (Ibata et al. 1997). For each of the  $q$  values of the dark halo potentials, we select orbits which have similar (mean) pericenter and apocenter distances as well as comparable  $L_z$  ( $z$ -component of the angular momentum) satisfying the above mentioned constraints. Our models of the dwarf are also slightly readjusted for each of the dark halo shapes, so as to produce the same remnant system by the present day. This implies that differences in the characteristics of the debris may only be attributed to a change in the flattening of the potential. The other possible free variables, such as the model of the dwarf and the orbital parameters, are (essentially) the same by construction.

We have studied five flattenings for the dark halo potential  $q = [0.8, 0.9, 1.0, 1.11, 1.25]$ , which correspond to average density axis ratios (within the orbit of Sgr)  $\langle q_\rho \rangle \sim [3/5, 4/5, 1, 5/4, 5/3]$ . In this Letter we focus on the properties of the satellite debris after 10 Gyr of evolution.

### 2.1. Young streams

We study now the characteristics of young debris streams. We select those particles that have been released by the dwarf in the last three pericentric passages (less than 2 Gyr ago in our models). The panels in Figure 1 show the heliocentric radial velocity vs. longitude  $\Lambda_{\text{sun}}$ <sup>3</sup> for this set of particles and for the different shaped dark halos. The large gray symbols in each of the panels correspond to the stars in Table 3 of M04 with distances is larger than 13 kpc. There appears to be very good

<sup>2</sup>It is worth noting that the isodensity surfaces are more oblate (prolate) than the equipotential surfaces.

<sup>3</sup>This variable corresponds to the angular distance along the stream. Its relation to  $(l, b)$  has been derived in Majewski et al. (2003)

<sup>1</sup>E-mail: ahelmi@astro.rug.nl

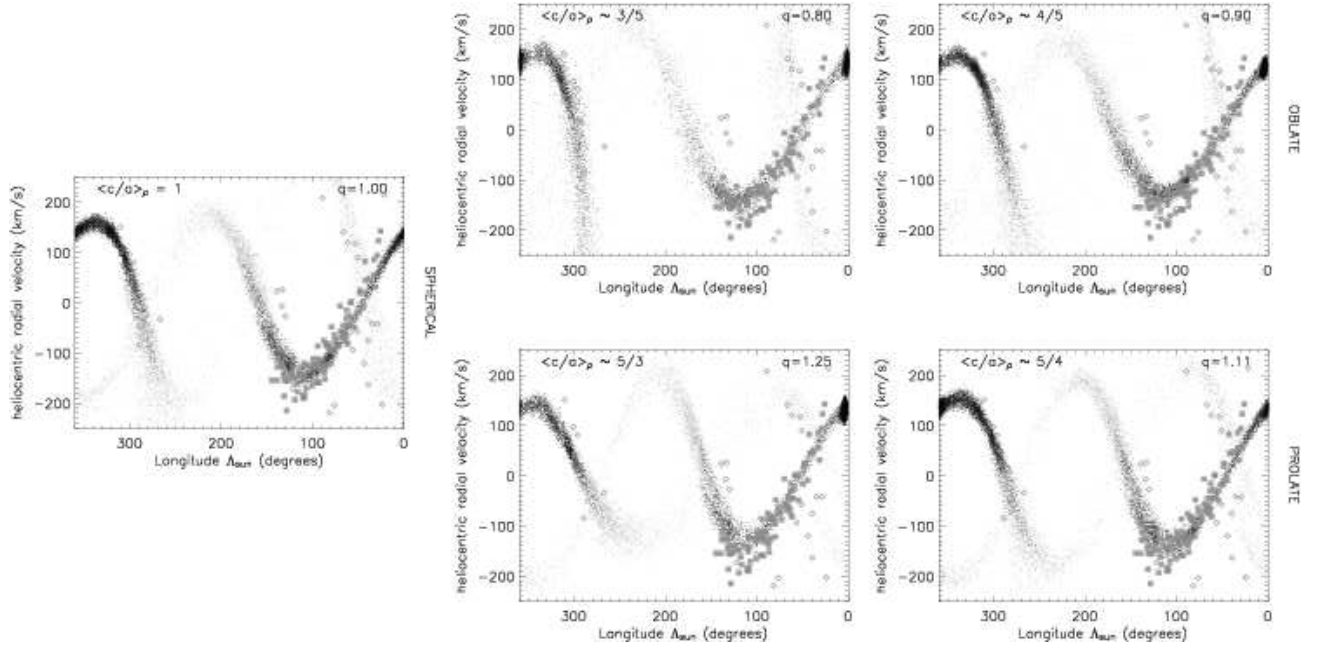


FIG. 1.— Distribution of  $(\Lambda_{\text{sun}}, V_r)$  for particles after 10 Gyr of evolution, for each one of the simulations with different degrees of flattening for the Galactic dark matter halo (black dots). Particles that have been released in the last 2 Gyr are shown in black, while the gray dots corresponds to those lost between 2 and 4 Gyr ago. The large gray symbols denote the stars observed by Majewski et al. (2004) with distances larger than 13 kpc, which is the criterion used by these authors to minimize the contamination by foreground thick disk and halo stars. Solid symbols correspond to stars which have been considered by M04 as likely members of the streams, while open symbols denote those that have been statistically identified as outliers by these authors. The (random) velocity errors quoted in Majewski et al. 2004 are  $\sim 6$  km/s.

agreement between the models and the stars in the streams of Sgr observed by M04.

To quantify how good the agreement is, we perform a  $\chi^2$  test. We bin the particles in the simulations (again only those lost in the last 3 pericentric passages) in elements of  $\Delta\Lambda_{\text{sun}} = 5^\circ$  width, and measure the mean radial velocity and the dispersion in each bin. We proceed in a similar way for the stars in M04 sample, selecting those that are more likely members of the stream as derived by M04 (these are the solid gray points in Figure 1). We then measure  $\chi^2$  as

$$\chi^2 = \sum_{i=1}^{N_{\text{bins}}} \frac{(\bar{V}_{i,o} - \bar{V}_{i,m})^2}{\sigma_{i,o}^2 + \sigma_{i,m}^2} \quad (2)$$

where  $\bar{V}_i$  is the mean radial velocity in the  $i$ th bin, and  $\sigma_i$  its dispersion. The subscripts  $o$  and  $m$  correspond to the observational data and to the model points, respectively. The results of this test are shown in Figure 2 and in the last column of Table 1.

Figure 2 confirms that in all cases, the models provide a good representation of the data: The value of the reduced  $\chi^2$  (which we defined as  $\chi^2/N_{\text{bins}}$ ) is close to unity. The most favored case (taken as that with the smallest  $\chi^2$ ) seems to be the most flattened halo  $q = 0.8$ . A bin to bin analysis of Figure 2 shows that the bin located at  $\Lambda_{\text{sun}} = 52.5^\circ$ , which contains only one data point, produces the largest deviation. If this star is removed, the  $\chi^2$  is significantly reduced for all shapes. In this case, the most favored models are those with  $q = 0.8$  ( $\langle c/a \rangle_\rho \sim 3/5$ ) and  $q = 1.25$  ( $\langle c/a \rangle_\rho \sim 5/3$ ). These correspond to the most oblate and to the most prolate halos we have considered.

We have also measured the  $\chi^2$  obtained by comparing models to models for the same range of longitude  $\Lambda_{\text{sun}}$  (see Table 1). We find that  $\chi^2$  is typically of the order of unity, and that the range in  $\chi^2$  values is the same as that obtained in the

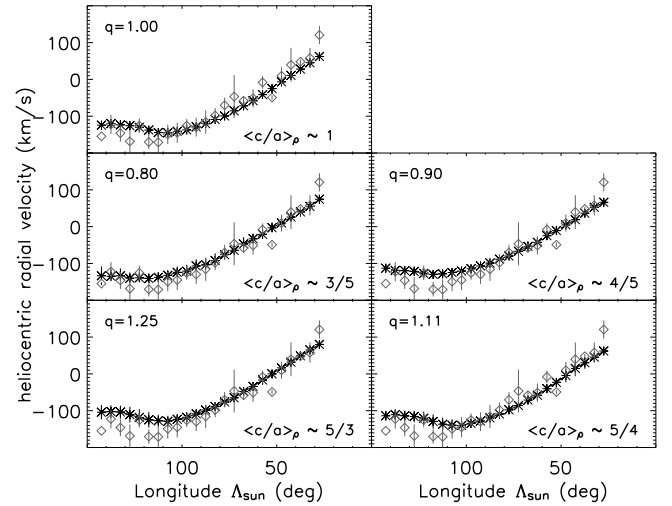


FIG. 2.— The predicted (asterisks) and observed (gray diamonds) distribution of mean heliocentric radial velocity measured in bins of  $\Delta\Lambda_{\text{sun}} = 5^\circ$  width, for the particles (in black) of Fig.1 and for the stars shown as filled gray symbols in the same figure.

data-models comparison. Small values of  $\chi^2$  are found for the comparison of model  $q = 0.8$  with  $q = 0.9$  and with  $q = 1.25$ , as well as for the comparison of  $q = 1.00$  with  $q = 1.11$ . This is most likely due to the fact that the sky projected orbital paths of the center of mass of Sgr overlap almost perfectly up to  $\Lambda_{\text{sun}} \sim 100^\circ$  for each of these two groups of models.

The extent of the stellar stream observed by M04 can be compared to our simulations to derive its age, i.e. the time elapsed since the stars became unbound from the Sgr dwarf. Since mass

loss preferentially occurs during pericentric passages, the age of a (portion of a) stream may also be measured by the number of pericentric passages that have passed since its formation. This quantity can easily be derived for the streams in our simulations. The material found in the range  $\Lambda_{\text{sun}} = [20^\circ, 150^\circ]$  has been lost in the last 3 passages:  $\sim 0.1$  Gyr ago (dominates close to the bound core),  $\sim 0.85$  Gyr ago and  $\sim 1.6$  Gyr ago (dominant at  $\Lambda_{\text{sun}} \gtrsim 100^\circ$ ). Uncertainties in this estimate can be attributed to incomplete knowledge of the orbit of the dwarf or of its mass-loss rate. The former, however, is well constrained by the available data (its average radial period lies in the range  $0.7 - 0.76$  in our models). The mass-loss rates are, on the other hand, constrained by the velocity dispersion found in the streams. Higher mass-loss rates than those found in these simulations would lead to thicker/hotter streams and at a given location, the stream will be younger. On the other hand, lower mass-loss rates would lead to colder structures (since the particles lost would have a smaller range of energies) which would be older on average. Inspection of Fig. 1 suggests that the uncertainty in the quoted values cannot be larger than  $\pm 1$  pericentric passage, that is  $\pm 0.75$  Gyr.

## 2.2. Older streams

How old do streams have to be before they show noticeable dissimilarities due to variation in the Galactic dark halo shape? The kinematics of particles lost between 2 and 4 Gyr ago (gray dots in Fig. 1) already exhibit important and measurable differences. These are further highlighted in Figure 3, which plots the trend in the heliocentric radial velocity as a function of longitude  $\Lambda_{\text{sun}}$  for three different cases:  $q = 0.8$  (light gray; diamonds),  $q = 1.00$  (dark gray; asterisks) and  $q = 1.25$  (black; triangles) for particles lost in the last 4 Gyr. The error bars indicate the expected velocity dispersion around the mean heliocentric radial velocity in a given longitude bin. The different models are clearly distinguishable at  $\Lambda_{\text{sun}} \sim 300^\circ$  in the trailing stream, and for  $\Lambda_{\text{sun}} \sim 240^\circ$  in the leading stream.

In fact Law et al. (2003) show in their Figure 1a, the radial velocities of a set of M giants from the 2MASS catalog located in the leading stream at  $\Lambda_{\text{sun}} = [200^\circ, 360^\circ]$ . We have digitized this plot (since the data are not yet available in tabular form) and show the corresponding data points as open squares in the top panel of Figure 4. The mean radial velocities measured as function of  $\Lambda_{\text{sun}}$  for the most oblate, the spherical and the most prolate models are overplotted for comparison. In order to reproduce the behavior of the radial velocity data around  $\Lambda_{\text{sun}} \sim 240^\circ$  in the leading stream, a prolate halo is required.

	0.90	1.00	1.11	1.25	DATA
0.80	0.177	0.706	0.679	0.276	<b>0.747 (0.401)</b>
0.90		0.938	0.678	0.269	<b>1.034 (0.726)</b>
1.00			0.061	1.461	<b>0.937 (0.797)</b>
1.11				1.101	<b>0.979 (0.806)</b>
1.25					<b>1.410 (0.621)</b>

TABLE 1

REDUCED  $\chi^2$  FOR THE DIFFERENT EXPERIMENTS. THE FIRST 4 COLUMNS ARE OBTAINED BY COMPARING THE DIFFERENT MODELS TO ONE ANOTHER. THE LAST COLUMN CORRESPONDS TO THE DATA TO MODEL  $\chi^2_{\text{red}}$ . THE VALUE BETWEEN BRACKETS IS OBTAINED WHEN THE BIN AT  $\Lambda_{\text{sun}} = 52.5^\circ$  IS NOT CONSIDERED.

A clear trend exists in the sense that the smaller the axis ratio of the dark halo, the more negative the mean galactocentric radial velocity at this location is, and hence, the less likely the model becomes. If the data in Law et al. (2003) are confirmed, this would be the *first direct evidence supporting a prolate shape for the dark halo of our Galaxy*.

While the  $q = 1.25$  model gives the best match to this new dataset, it seems clear that an even more elongated halo could yield a better fit. Another option could be to reduce the mass of the disk by a small amount while keeping this axis ratio fixed. We explore these two possibilities using test particle orbits. The results are presented in the bottom panel of Figure 4 for the longitudes probed by the leading and trailing streams traced so far. The black curves correspond to our original set of parameters:  $M_{\text{disk}} = 10^{11} M_\odot$ ,  $v_{\text{halo}} = 131.5$  km/s, and  $d = 12$  kpc, for the cases  $q = 1$  (dashed),  $q = 1.25$  (solid) and  $q = 1.5$  (dotted). The dark gray curves have been computed with a lower disk mass  $M_{\text{disk}} = 5 \times 10^{10} M_\odot$ , while keeping the  $v_{\text{LSR}}$  and the circular velocity at 200 kpc fixed (this changes  $v_{\text{halo}} = 137$  km/s and  $d = 3.5$  kpc). Therefore we conclude that reducing the mass of the disk has a negligible effect on the orbital path. Moreover, the very prolate  $q = 1.5$  halo seems to be too elongated and does not trace well the trends in the data shown in the top panel of Figure 4.

## 3. SUMMARY

There is good agreement between the models and the stars in the trailing stream of Sgr observed by M04. The comparison confirms that the different models can scarcely be distinguished from one another when only the dynamics of the youngest streams ( $\lesssim 1.6$  Gyr of age) are analyzed, since all of them reproduce to similar extent the radial velocity trends observed in the data.

To make reliable estimates of the shape of the dark halo of the Galaxy slightly older streams are needed. The Sgr leading stream data published by Law et al. (2003) encompass such

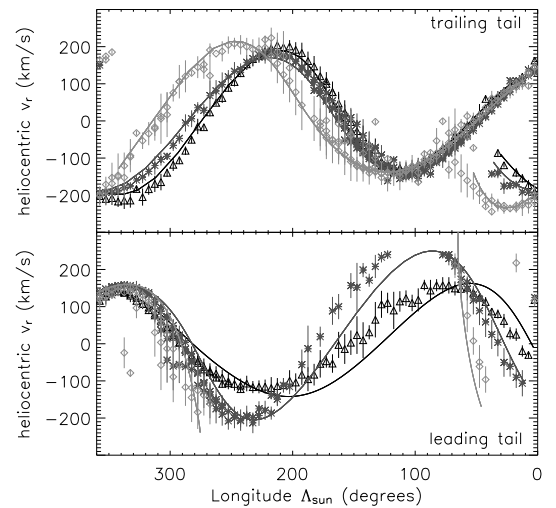


FIG. 3.— The predicted mean heliocentric radial velocity measured in bins of  $\Delta\Lambda_{\text{sun}} = 5^\circ$  width, for particles lost in the last 4 Gyr for models with  $q = 0.8$  (light gray, diamonds),  $q = 1.00$  (dark gray, asterisks) and  $q = 1.25$  (black, triangles). The solid curves indicate the actual trajectory followed by the center of mass in the simulations. Note that while the overall behavior of the latter is similar, the actual mean value at each longitude bin can be quite different. The error bars indicate the velocity dispersion around the mean in each bin.

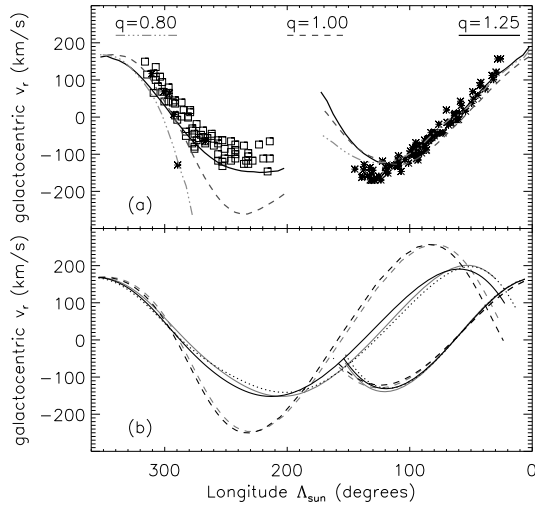


FIG. 4.— *Panel (a)*: The predicted mean galactocentric radial velocity vs  $\Lambda_{\text{sun}}$  measured in bins of  $\Delta\Lambda_{\text{sun}} = 5^\circ$  width, for particles lost in the last 4 Gyr of evolution for models with  $q = 0.8$  (light gray; dot-dashed),  $q = 1.00$  (dark gray; dashed) and  $q = 1.25$  (black; solid). The asterisks correspond to the data published by M04, while the open squares are from Law et al. (2003). *Panel (b)*: The galactocentric radial velocity vs  $\Lambda_{\text{sun}}$  for test particle orbits integrated in different potentials:  $q = 1$  (dashed),  $q = 1.25$  (solid) and  $q = 1.5$  (dotted). The black curves correspond to the original parameters, while the dark gray to halving the disk mass.

older debris ( $\sim 2 - 4$  Gyr of dynamical age). This dataset strongly suggests that the dark halo of the Milky Way is prolate and that the average density axis ratio  $\langle c/a \rangle_\rho$  within the orbit of Sgr is probably larger than  $5/3$  ( $q = 1.25$ ) but smaller than  $12/5$  ( $q = 1.5$ ).

This result has a range of important implications. It rules out models in which the dark matter is distributed as the baryons in our Galaxy, such as for example in the form of cold  $H_2$  clumps in the outer disk (e.g. Pfenniger & Combes, 1994). Moreover, it poses a big problem for MOND because requires the MOND force field – which depends on the (oblate) distribution of luminous matter in the Galaxy – to mimic the gravitational effect of a prolate halo. Finally, a prolate shape could go a long way in explaining the Holmberg effect (e.g. Sales & Garcia-Lambas 2004): the excess of satellites observed along the minor axis of disk galaxies may just be reflecting the shape of the underlying mass distribution.

I would like to thank Heather Morrison, Paul Harding, Ed Olszewski, Simon White and Mariano Mendez for very enjoyable discussions, and the anonymous referee for a very constructive report.

#### REFERENCES

- Bullock, J. S. 2002, in Proceedings of the Yale Cosmology Workshop “The Shapes of Galaxies and Their Dark Matter Halos”, ed. P. Natarajan (Singapore: World Scientific), 109  
 Helmi, A. 2004, MNRAS (in press), astro-ph/0309579  
 Ibata, R., Wyse, R., Gilmore, G., Irwin, M., & Suntzeff, N. 1997, AJ, 113, 634  
 Ibata, R., Lewis, G., Irwin, M., Totten, E., & Quinn, T. 2001, ApJ, 551, 294  
 Johnston, K. V., Spergel, D. N., & Hernquist, L. 1995, ApJ, 451, 598  
 Law, D. R., Majewski, S. R., Johnston, K. V., & Skrutskie, M. F. 2003, in Proc. of “Satellites and tidal streams”, eds. F. Prada and D. Martinez-Delgado, in press (astro-ph/0309567)  
 Majewski, S.R., Skrutskie, M.F., Weinberg, M.D., & Ostheimer, J.C. 2003, ApJ, 599, 1082

- Majewski S., et al. 2004, ApJ, (in press), astro-ph/0403701  
 Milgrom, M. 2001, MNRAS, 326, 1261  
 Pfenniger, D., & Combes, F. 1994, A&A, 285, 94  
 Sales, L., & Garcia-Lambas, D. 2004, MNRAS, 348, 1236